JOURNAL OF APPLIED ELECTROCHEMISTRY 16 (1986) 490–504

The dissolution and passivation of polycrystalline iron electrodes in boric acid–borate buffer solutions in the 7.5–9.2 pH range

M. E. VELA, J. R. VILCHE, A. J. ARVIA

Instituto de Investigaciones Fisicoquímicas Teóricas y Aplicadas – INIFTA, Casilla de Correo 16, Sucursal 4, 1900 La Plata, Argentina

Received 18 April 1985; revised 18 June 1985

The voltammetric responses of iron in boric acid–borate buffer solutions in the 7.5–9.2 pH range and 0–75° C range show two different and successive stages related to passivation. The first electro-oxidation stage leading to passivity onset corresponds to $Fe(OH)_2$ electroformation. The second stage corresponds to the growth and second level electro-oxidation of the prepassive layer.

A reaction mechanism accounting for the electroformation and electroreduction of the $Fe(OH)_2$ layer is discussed. A duplex passive layer structure involving an inner layer with a Fe_3O_4 limiting structure at high positive potential and an outer hydrous iron oxy-hydroxide layer seems adequate for understanding the experimental data.

1. Introduction

In the last two decades the metal dissolution and active-to-passive transition in relation to the nature of the prepassivating and passivating films on polycrystalline iron electrodes in borate buffer solutions have been extensively studied [1–34]. Cohen and co-workers [1–6] admitted the existence of some Fe_3O_4 on the surface in the active potential region, whereas the structure of the film in the passive region was interpreted in terms of an inner Fe_3O_4 layer and an outer γ-Fe_2O_3 layer, the passivation potential being governed by the γ-Fe_2O_3/Fe^{2+} equilibrium reaction. The presence of ferrous ions leads to the additional formation of a mixed hydrated iron–boron–oxygen compound of amorphous nature [5].

Kruger and co-workers [7, 8] found a Fe_3O_4-spinel-like structure in the prepassive potential range and the presence of γ-Fe_2O_3 in all passive films and suggested that the initial film growth process was controlled by diffusion to the surface. According to Moshtev [9, 10] the sharp pseudocapacitance drop at passivity indicated complete γ-Fe_2O_3 surface coverage.

In a series of papers, Sato and co-workers [11–19] investigated the structure, composition and thickness of passive films formed on iron in borate solutions in the 6.0–11.5 pH range by means of cathodic reduction combined with ellipsometry and chemical analysis and by Auger analysis. According to these results the passive film consists of an inner barrier layer generated by a direct electro-oxidation of metallic iron, and an outer deposit layer formed by anodic oxidation of ferrous ion dissolved from the iron electrode during the initial period of passivation. In the potential region where passivity is still incomplete, both Fe(II) and Fe(III) species were detected in the poorly hydrated barrier layer and in the hydrated deposit layer. The amount of Fe(II) species included in these layers decreases as either the potential increases or the pH decreases. In the passive region only Fe(III) species are apparently present in the two layers, probably as Fe_2O_3 at the barrier layer and as $Fe(OH)_3$ at the deposit layer.

Results reported by Ord and co-workers [20–26], covering a wide range of experimental

0021–891X/86 $03.00 + .12 © 1986 Chapman and Hall Ltd.

conditions, were also explained in terms of a duplex film whose component layers undergo simultaneous growth during passive-state oxidation. A thin inner layer is already grown in the active state before formation of the outer layer and the electrode passivity implies only a monolayer fraction of the outer film on the surface. Experiments performed without removing Fe(II) ions produced on passivation reveal that a FeOOH layer can be deposited at potentials above the FeOOH deposition potential.

According to Bockris *et al.* [27, 28], transient ellipsometric data give evidence that the initial phase oxide, probably $Fe(OH)_2$, grows before the current–potential peak in the passivation, being the phase oxide thickness at the peak potential of about a monolayer. When the potential of the current peak is exceeded, the $Fe(OH)_2$ species is converted to Fe_2O_3. The passive layer which grows at higher anodic potentials contains Fe(III) species. Data from various high-vacuum spectroscopic techniques favour an amorphous hydrated polymeric oxide model [29–32], where the bound water is essential for cementing the polymeric iron oxide chains in the passive film.

Recent results on freshly generated iron surfaces in borate solutions [33, 34] suggest that the formation of an adsorbed layer of FeOH takes place by random oxidation of exposed metal atoms at potentials below the Fe/Fe(II) reversible potential. Similar conclusions have been derived by using the triangularly modulated triangular potential sweep technique from the transient response of iron in either strong alkaline [36, 37] or slight acid [38] solutions. Furthermore, steady-state results of the anodic dissolution of iron in borate buffer solutions were also explained by a branching mechanism with the assumption that the degree of surface coverage by FeOH species approaches one [39].

The present paper deals with the kinetics and mechanism of active to passive transition of iron in buffered borate electrolytes, in particular to obtain electrochemical evidence of the different properties of prepassive and passive films and to correlate possible passive layer structures with optical data already reported in the literature.

2. Experimental details

Working electrodes consisting of either fixed wires (0.5 mm diameter, 0.25 cm^2 apparent area) or circular plane rotation discs (0.070 cm^2 apparent area) of polycrystalline iron ('Specpure', Johnson Matthey Chemicals Ltd) mounted in Teflon holders were used. They were gradually polished starting with 400 and 600 grade emery papers and finishing with 0.3 and 0.1 μm alumina–acetone suspension. Finally, the electrodes were cleaned with acetone and repeatedly washed with thrice-distilled water. A three-compartment electrolysis Pyrex cell was employed. Electrode potentials were measured against a saturated calomel electrode (SCE) although potentials in the text are referred to the NHE scale. The reference electrode was mounted with the usual Luggin–Haber capillary tip and fritted glass disc to prevent chloride ion diffusion into the electrolyte solution. A large-area platinum sheet was employed as counter electrode.

The following electrolyte solutions were used: 0.075 M $Na_2B_4O_7$ + z M H_3BO_3, with $0.15 \leqslant z \leqslant 0.60$ corresponding to $9.2 \geqslant$ pH $\geqslant 7.5$ buffered solutions. These were prepared from thrice-distilled water and analytical grade (Merck) reagents. Runs were made in the 0–75° C temperature range under purified H_2 gas saturation with both still and stirred solutions at different rotation speeds (w). Before each measurement the polished electrode was held for 5 min at a potential at which H_2 evolution took place. Experiments were performed using single (STPS), repetitive (RTPS) and triangularly modulated (TMTPS) triangular potential sweeps between present cathodic ($E_{s,c}$) and anodic ($E_{s,a}$) switching potentials at a sweep rate v($0.001\,V\,s^{-1} \leqslant v \leqslant 0.5\,V\,s^{-1}$).

3. Results

The stabilized voltammograms of iron in still solution at pH 9.2 and 25° C run between $E_{s,c} = -0.99$ V and $E_{s,a} = 1.14$ V exhibit four main anodic current contributions (I, II, III and III′) and

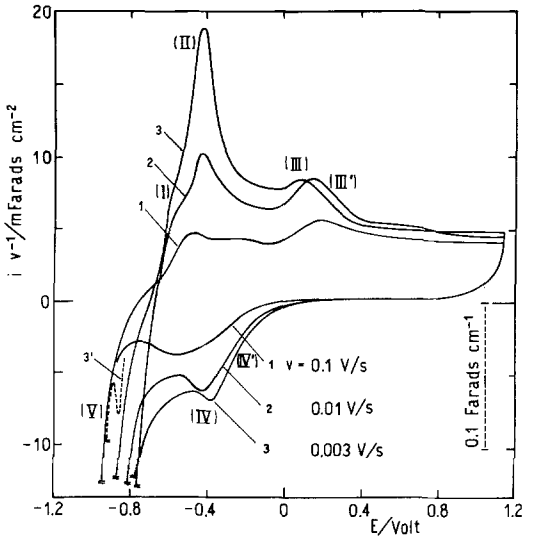

Fig. 1. Influence of v on the voltammograms run between $E_{s,c} = -0.99$ V and $E_{s,a} = 1.14$ V at pH 9.2, 25° C.

three cathodic current contributions (IV', IV and V). Peak V overlaps the contribution of the H_2 evolution reaction (Fig. 1). The nomenclature of the peaks follows that used in previous publications referred to the same subject in alkaline media [40–42]. The stabilized voltammograms are obtained after 10–15 cycles and the reproducibility of the electrochemical response is very good provided that the potential cycling is preceded by a holding of the potential at $E_{s,c}$ (just in the H_2 evolution potential range) for 5 min to electroreduce the iron surface. Under these conditions the potential cycling produces practically no change in the shape of the voltammogram except for a small decrease in charge, lower than 10%, in going from the first voltammogram to the stabilized one. The voltammogram in the pseudocapacitance versus potential display shows that the relative distribution of peaks depends on v, particularly in the negative potential region, and the lower the value of v the steeper the pseudocapacitive peaks. When the potential applied to the electrode is more positive than 0.4 V (passive range) the pseudocapacitive current becomes practically independent of v.

The reactions taking place in the potential range of peaks I and II yield species which are electroreduced at the potential range of peak V (Fig. 2). This is clearly seen by stepwise changing $E_{s,a}$ in the potential range of peak II. When $E_{s,a}$ exceeds 0 V, the contribution of peak IV is seen in

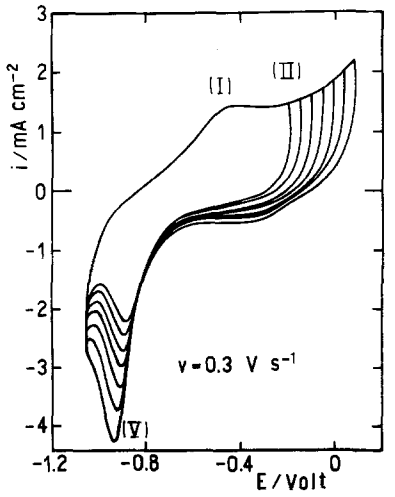

Fig. 2. Influence of $E_{s,a}$ on the electroreduction voltammograms in the potential range of peak II. $E_{s,c} = -1.05$ V, pH 9.2, 25° C.

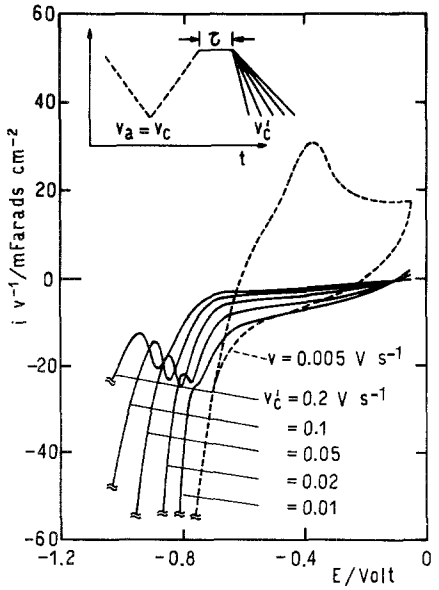

Fig. 3. Voltammetric response obtained with the perturbation programme depicted in the figure. Influence of v_c on the electroreduction E–i profiles after a potential holding at $E_{s,a}$ during τ = 5 m. The iron electrode was previously subjected to RTPS at $v = 0.005\,V\,s^{-1}$ between $E_{s,c} = -1.06$ V and $E_{s,a} = -0.06$ V to obtain the stabilized E–i profile, pH 9.2, 25° C.

the electroreduction scan. The dependence of the electroreduction profiles on the cathodic sweep rate (v_c) was studied by forming the anodic layer at a constant anodic sweep rate (v_a), $v_a = 0.005\,V\,s^{-1}$, and holding the potential at $E_{s,a}$ for τ = 5 min (Fig. 3). In the $0.005\,V\,s^{-1} \leqslant v_c \leqslant 0.2\,V\,s^{-1}$ range the height of peak V ($i_{p,V}$) increases linearly with $v_c(\partial \log i_{p,V}/\partial \log v_c)_{v_a,\tau} = 1$, and its potential ($E_{p,V}$) shifts towards more positive values fitting a linear $E_{p,V}$ versus $\log v_c$ plot with slope $(\partial E_{p,V}/\partial \log v_c)_{v_a,\tau} = -0.10$ V per decade.

Conjugated current peaks I–II/V can be assigned to the Fe(0)/Fe(II) redox system as for the case of iron electrodes in concentrated alkaline solutions [40, 43, 44]. The voltammetric reversibility of this reaction decreases as $E_{s,a}$ is made more positive, probably because the reaction product undergoes irreversible chemical changes. The strong dependence of the voltammogram on $E_{s,a}$ (Fig. 4) reflects particularly in the distribution and location of the electroreduction current peaks. When $E_{s,a}$ exceeds 0.4 V, the coupling of the group of peaks III–III′ with the group of peaks IV–IV′ can be established. The electro-oxidation level achieved during the negative potential going excursion depends on $E_{s,c}$ and v_c (Fig. 5) and the shape of the electro-oxidation profile depends also on

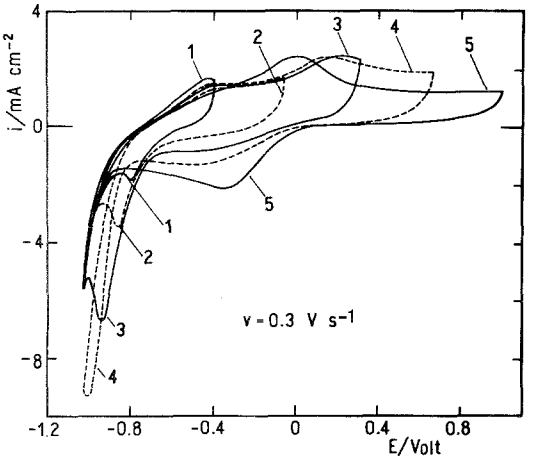

Fig. 4. Voltammograms obtained at $0.3\,V\,s^{-1}$ between $E_{s,c} = -1.03$ V and $E_{s,a}$ changed stepwise either up or down at pH 9.2, 25° C. Values of $E_{s,a}$: curve 1, −0.40 V; curve 2, −0.05 V; curve 3, 0.31 V; curve 4, 0.72 V; curve 5, 1.02 V.

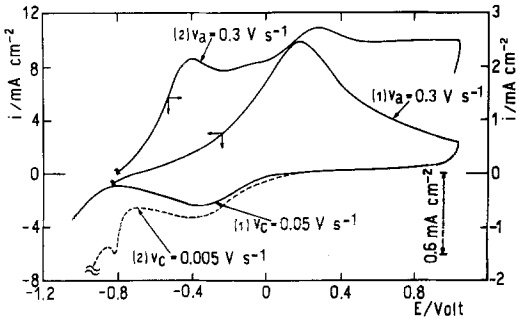

Fig. 5. Influence of v_c on the voltammograms run with asymmetric RTPS between $E_{s,c} = -1.06$ V and $E_{s,a} = 1.04$ V, $v_a = 0.3\,V\,s^{-1}$. The electrode was previously perturbed with symmetric RTPS, $v_a = v_c = 0.3\,V\,s^{-1}$ to attain the stabilized E–i profile. Curve 1, $v_c = 0.05\,V\,s^{-1}$; curve 2, $v_c = 0.005\,V\,s^{-1}$. pH 9.2, 25° C.

the preceding voltammetric excursion. When $E_{s,a} = -1.06$ V and $v_c = 0.005\,V\,s^{-1}$ (Fig. 5, curve 2) the electro-oxidation profile at $v_a = 0.3\,V\,s^{-1}$ shows peaks I, II and III, while at $v_c = 0.05\,V\,s^{-1}$ only peak III is noticed (Fig. 5, curve 1). These results confirm that different electroreduction levels are achieved according to the perturbation conditions. This fact can be regarded as a consequence of the composite structure of the passivating layer either whether it is formed of a mixture of various species or the composition changes in depth.

The voltammetric charge of peak I up to the peak potential value (Fig. 6) is about 0.95 mC cm^{-2} and independent of v (Fig. 7). On the assumption that the voltammetric contour of peak I is symmetric, the total voltammetric charge should be about 1.8–2.0 mC cm^{-2}. This charge can be predominantly assigned to the formation of the $Fe(OH)_2$ layer. If it is assumed that only a monolayer of $Fe(OH)_2$ is formed and that the above mentioned charge is compared with the monolayer charge reported for metal hydroxides, $Me(OH)_2$, where Me = Fe, Co or Ni, estimated between 0.66 and 0.70 mC cm^{-2} [45, 46], one may conclude that the roughness factor of the iron electrode in the boric acid–sodium borate electrolyte is about three. Conversely, if it is considered that the roughness factor is equal to one, then the greatest thickness of the $Fe(OH)_2$ layer should reach that of about three monolayers. The assumption that the anodic reaction in the potential range of peak I corresponds to the formation of the $Fe(OH)_2$ layer is in agreement with the results obtained for iron in concentrated base [40, 47] and slightly acid [38, 48, 49] electrolytes. The voltammetric charge up to the peak potential value for peak V is also about 0.95 mC cm^{-2} (Fig. 7) provided that $E_{s,a}$ is adjusted to cover the voltammetric oxidation level of peak I (Fig. 6).

At pH values 8.4 and 7.5 the same voltammetric response of iron as in boric acid–sodium borate solution at pH 9.2 is observed. In the 7.5–9.2 pH range the charge of peak I is independent of pH. The kinetic parameters of peaks I and V derived from the voltammetric relationships in the

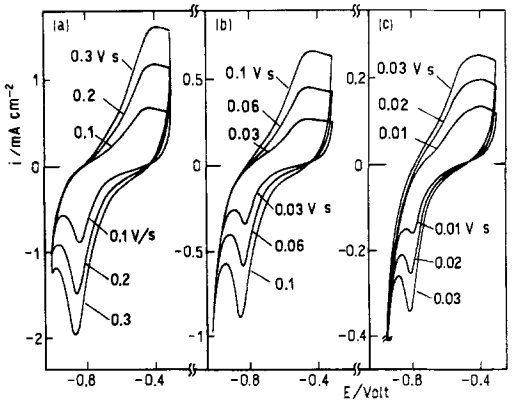

Fig. 6. Influence of v on the voltammograms run between $E_{s,c} = -1.01$ V and $E_{s,a} = -0.31$ V at pH 9.2, 25° C.

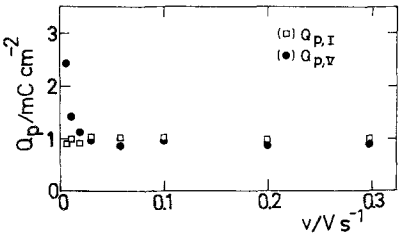

Fig. 7. Influence of v on the voltammetric charge measured up to the potential of peaks I and V, under conditions of Fig. 6. □, $Q_{p,I}$; ●, $Q_{p,V}$.

$0.002\,V\,s^{-1} \leqslant v \leqslant 0.3\,V\,s^{-1}$ range (Figs 8–12) can be summarized as follows:

$$\left(\frac{\partial E_{p,I}}{\partial \log v}\right)_{pH} = 0.065 \pm 0.008\,V \text{ per decade}; \qquad \left(\frac{\partial \log i_{p,I}}{\partial \log v}\right)_{pH} = 0.88 \pm 0.07$$

$$\left(\frac{\partial E_{p,I}}{\partial pH}\right)_{v} = -0.051 \pm 0.007\,V; \qquad \left(\frac{\partial \log i_{p,I}}{\partial pH}\right)_{v} = 0 \pm 0.1$$

$$\left(\frac{\partial E_{p,V}}{\partial \log v}\right)_{pH} = -0.063 \pm 0.007\,V \text{ per decade}; \qquad \left(\frac{\partial \log i_{p,V}}{\partial \log v}\right)_{pH} = 0.86 \pm 0.08$$

$$\left(\frac{\partial E_{p,V}}{\partial pH}\right)_{v} = -0.058 \pm 0.006\,V; \qquad \left(\frac{\partial \log i_{p,V}}{\partial \log v}\right)_{v} = 0 \pm 0.1$$

The linear dependence of $E_{p,I}$ on pH is also fitted by results obtained with other electrolytes in the $6.5 \leqslant pH \leqslant 14$ range, $(\partial E_{p,I}/\partial pH)_v = -0.064 \pm 0.009\,V$ (Fig. 10).

The height of peak I and its voltammetric charge are practically temperature independent in the $0°\,C \leqslant T \leqslant 75°\,C$ range.

In the potential range of peak II the anodic layer continues to grow and, accordingly, its electroreduction becomes more difficult as peak V shifts towards more negative potential values. This suggests that the growth of the anodic layer at more positive potentials implies not only an increase in charge but also a gradual structural change probably associated with the progressive loss of water and protons from the bulk of the layer. Both the height ($i_{p,II}$) and potential ($E_{p,II}$) of peak II change linearly with $v^{1/2}$ (Fig. 13) as predicted for the growth of the anodic layer under ohmic resistance polarization control [50, 51]. The values of $i_{p,II}$ and $E_{p,II}$ extrapolated to $v = 0$ depend on pH and temperature. At pH 9.2 and 25° C, the corresponding values are $(i_{p,II})_{v=0} = 0.045\,mA\,cm^{-2}$ and $(E_{p,II})_{v=0} = -0.34\,V$, respectively. In the $0°\,C \leqslant T \leqslant 75°\,C$ range, $i_{p,II}$ fits an Arrhenius plot (Fig. 14) and the corresponding apparent activation energy is 2.9 kcal mol^{-1} at any value of v. On the other hand, the temperature coefficient of $(E_{p,II})_{v=0}$ is $2\,mV\,K^{-1}$ (Fig. 15).

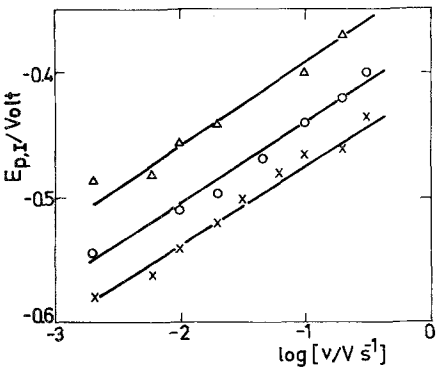

Fig. 8. Dependence of $E_{p,I}$ on v at 25° C. x, pH 9.2; ○, pH 8.4; △, pH 7.5.

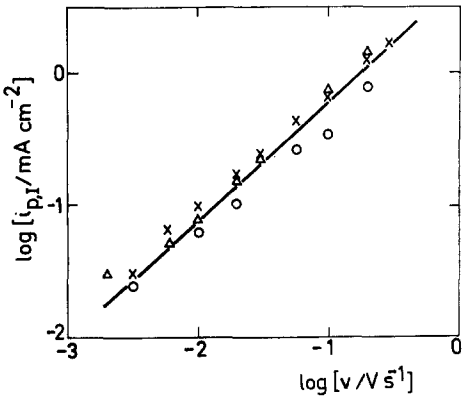

Fig. 9. Dependence of $i_{p,I}$ on v at 25° C. x, pH 9.2; o, pH 8.4; △, pH 7.5.

The range of TMTPS parameters for obtaining detailed TMTPS voltammograms is rather limited because of the large overlapping of the different processes which, as already mentioned, exhibit a different dependence of v. Notwithstanding, the TMTPS voltammogram in the potential range of peaks I and V (Fig. 16) confirms the assignment of conjugated current peaks referred to above. The change of the slope of the current–potential profile of each modulating scan shows that the reversibility of the processes depends considerably on the potential range considered. Reactions appear more reversible in the neighbourhood of the potential peaks. On the other hand, the TMTPS voltammograms in the -1.0 V to 0.8 V range for the range of amplitude of the modulating potential, $\Delta E_m = 0.2$ V (Fig. 17) show multiple peaks which can be taken as an indication of various intermediate stages related to the overall reactions revealed by the type of potential perturbation applied to the electrode [36–38].

4. Discussion

4.1. *Reactions related to the initial passivation stage*

The kinetics of iron electrode reactions in aqueous solution have been explained through different mechanisms usually postulated on the basis of conventional chemical kinetics involving the participation of reactants and products of defined stoichiometry [52, 53]. It is generally accepted that the iron electro-oxidation reaction implies a complex reaction mechanism where the first stage is the formation of $Fe(OH)_{ad}$ species through the reversible underpotential decomposition of water, but the following stage finally yielding Fe(II) and Fe(III) species are only ambiguously established. However, at present there are sufficient electrochemical [33–42, 47–49, 52, 53], optical [27, 28, 54,

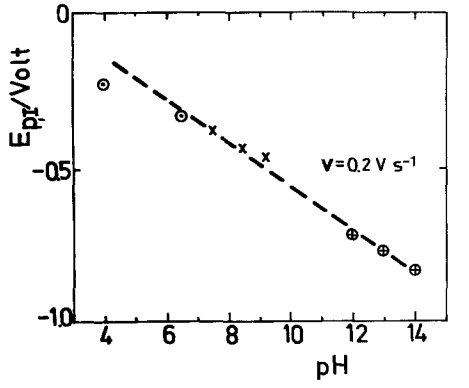

Fig. 10. Dependence of $E_{p,I}$ on pH derived from the voltammograms run at $v = 0.2$ V s^{-1} at 25° C in the following solutions: x, borate–boric acid solutions, pH = 7.5, 8.4, 9.2; ⊕, potassium hydroxide solutions [36, 37, 40, 41], pH = 12.0, 12.9, 13.9; ⊙, neutral and slightly acid solutions containing potassium sulphate [38], pH = 4.0, 6.5.

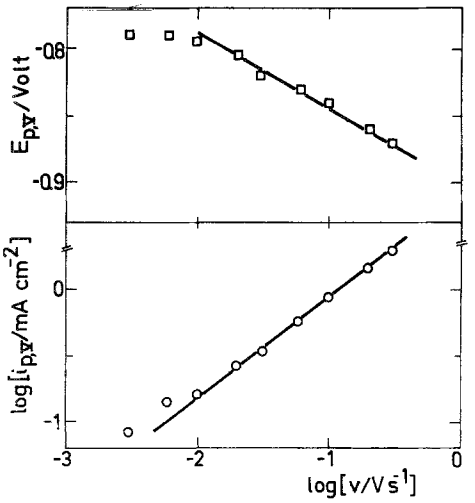

Fig. 11. Dependence of $i_{p,V}$ and $E_{p,V}$ on v from voltammograms obtained under RTPS conditions between $E_{s,c} = -1.01$ V and $E_{s,a} = -0.31$ V at pH 9.2, 25° C.

55] and thermodynamic [19] data which support the view that in base solution the stable species corresponding to the first oxidation level of iron is $Fe(OH)_2$. Therefore the voltammetric current peak I, resulting from iron in the boric acid–sodium borate solution, is assigned to the formation of a thin hydrous $Fe(OH)_2$ layer. In the potential range of peaks I and II it is reasonable to expect that a fraction of the voltammetric charge can be also related to the formation of soluble Fe(II). On the other hand the interpretation of the voltammetric results indicate that the complementary electroreduction of $Fe(OH)_2$ is associated with peak V. The kinetic parameters derived for peak I and V can be reasonably explained through a relatively simple reaction pathway.

4.2. *Probable reaction pathway for $Fe(OH)_2$ electroformation and electroreduction*

There is evidence from nuclear microanalysis using stable oxygen isotopes that the surface of iron maintained under cathodic polarization is free of oxygen [56]. Therefore the initial step of the iron

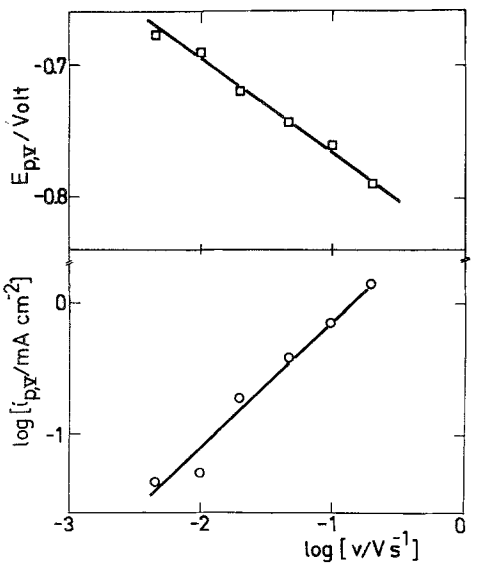

Fig. 12. Dependence of $i_{p,V}$ and $E_{p,V}$ on v from voltammograms run under RTPS conditions between $E_{s,c} = -0.96$ V and $E_{s,a} = -0.24$ V at pH 7.5, 25° C.

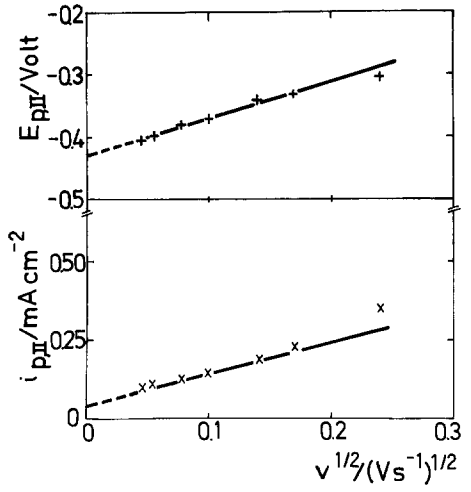

Fig. 13. Dependence of $i_{p,II}$ and $E_{p,II}$ on $v^{1/2}$ from voltammograms run under RTPS conditions between $E_{s,c} = -1.06$ V and $E_{s,a} = 0.04$ V at pH 9.2, 25° C.

electro-oxidation in slightly alkaline solution can be written as two equivalent processes, namely:

$$[Fe] + H_2O = [Fe](H_2O)_{ad} \quad (1a)$$

$$[Fe](H_2O)_{ad} = [Fe(OH)_{ad}] + H^+ + e \quad (1b)$$

and

$$[Fe] + OH^- = [Fe](OH^-)_{ad} \quad (2a)$$

$$[Fe](OH^-)_{ad} = [Fe(OH)_{ad}] + e \quad (2b)$$

Reactions 1a and b correspond to the adsorption of water and its electro-oxidation yielding adsorbed OH. Brackets and parentheses denote species at the electrode surface and adsorbed species, respectively. Reactions 2a and b indicate the formation of adsorbed OH through the adsorption of OH^- ion. The relative contribution of these reactions depends on the pH of the solution but, in any case, the electron transfer processes are sufficiently fast either in acid, neutral or base electrolyte solutions [33–39, 52, 53]. Atom superposition and electron delocalization molecular orbital calculations made for the adsorption and reaction of single H_3O^+, H_2O and OH molecules on an Fe_5 model for an iron electrode over the intermediate potential range between H_2 and O_2 formation show that H_2O is found to dehydrogenate creating a surface OH species [57].

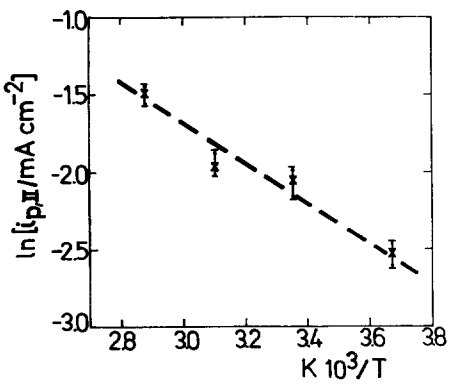

Fig. 14. Arrhenius plot of $i_{p,II}$; $v = 0.01$ V s^{-1}; pH 9.2, 25° C.

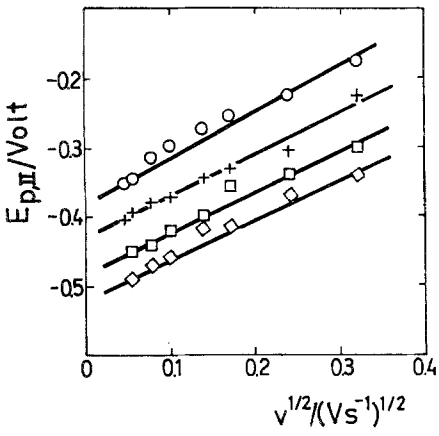

Fig. 15. Dependence of $E_{p,II}$ on $v^{1/2}$ from voltammograms at pH 9.2 and different temperatures. ○, 0° C; +, 25° C; □, 50° C; ◇, 75° C.

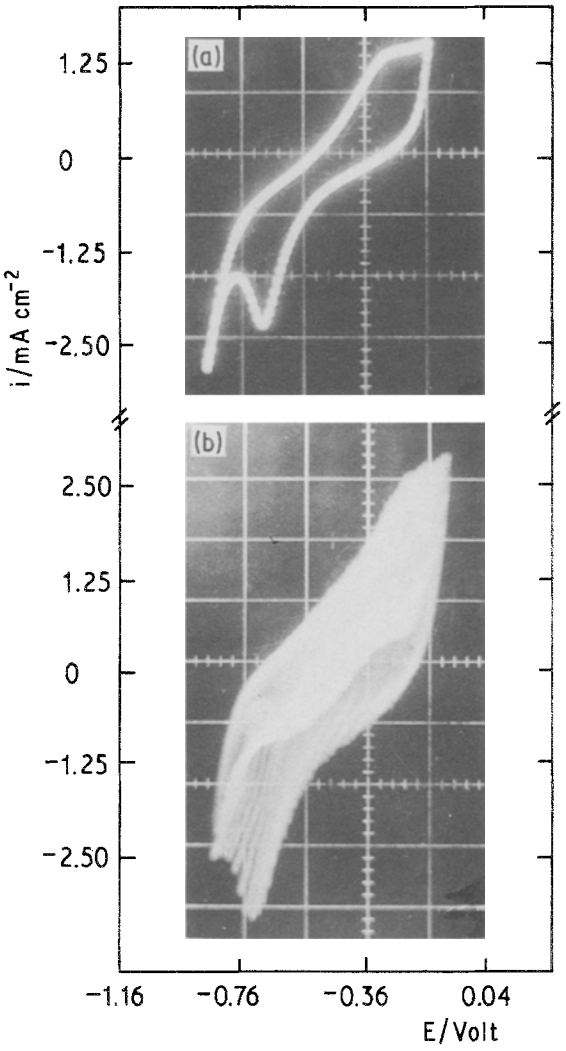

Fig. 16. Comparison between RTPS and TMTPS voltammograms at pH 8.4, 25° C. (a) $v = 0.5\,V\,s^{-1}$; (b) $v_b = 0.5\,V\,s^{-1}$, $v_m = 8\,V\,s^{-1}$, $\Delta E_m = 0.15\,V$.

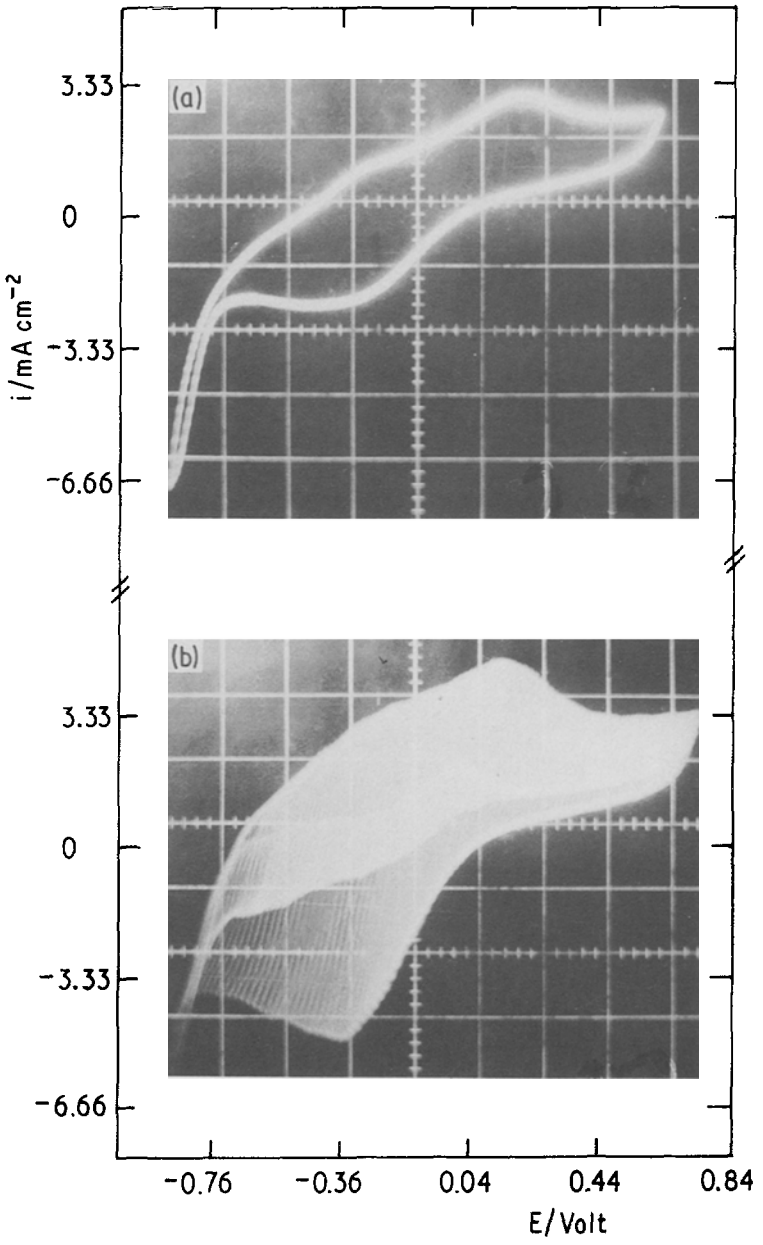

Fig. 17. Comparison between RTPS and TMTPS voltammograms at pH 8.4, 25°C. (a) $v = 0.5\,V\,s^{-1}$; (b) $v_b = 0.5\,V\,s^{-1}$, $v_m = 10\,V\,s^{-1}$, $\Delta E_m = 0.2\,V$.

The $Fe(OH)_{ad}$ species can be formed up to a limiting amount which would correspond to the complete coverage of the iron surface. During this process the layers of water molecules adjacent to the electrode have to be rearranged, because of the formation of the $[Fe(OH)_{ad}]$ surface dipoles. This implies that the structure of the interface acquires a minimum energy compatible with the equilibrium condition at each potential. The corresponding energy change assists a surface chemical reaction such as a rearrangement step involving $Fe(OH)_{ad}$ species and adjacent water (n and n') as represented by the following reaction:

$$[Fe(OH)_{ad}]nH_2O \xrightarrow{k_3} Fe(OH)_{ad}]^*n'H_2O + (n - n')H_2O \qquad (3)$$

where the asterisk denotes another configuration of the reaction intermediate at the electrode

surface. The new species becomes energetically favoured to participate in the second charge transfer step yielding hydrous $Fe(OH)_2$ according to a reaction such as

$$[Fe(OH)_{ad}]^* n'H_2O + OH^- = [\text{hydrous } Fe(OH)_2] + e \quad (4)$$

The hydrous $Fe(OH)_2$ layer can be considered to be mainly responsible for the prepassivation of iron in boric acid–sodium borate solution. Depending on the solution pH, hydrous $Fe(OH)_2$ participates in the following ionic equilibria [58]:

$$Fe(OH)_2 + OH^- = Fe(OH)_3^- \quad (5a)$$

$$Fe(OH)_2 + 2OH^- = Fe(OH)_4^{2-} \quad (5b)$$

$$Fe(OH)_2 = Fe(OH)^+ + OH^- \quad (5c)$$

$$Fe(OH)_2 = Fe^{2+} + 2OH^- \quad (5d)$$

The relative contribution of each reaction depends on the pH of the solution.

In the prepassive potential region, Frankenthal [59] proposed a dissolution–adsorption mechanism in which the iron dissolution proceeds by the direct, activated transfer of ions from the metal into solution.

From the kinetic standpoint, Reaction 3 can be considered as the rate determining step and, in addition, it can be assumed that the hydrous $Fe(OH)_2$ layer grows homogeneously. Thus under the experimental conditions of the present work, from the reversible characteristics of the first step, either Reaction 1 or 2 under Langmuir adsorption conditions, one can write:

$$k_+ c_{OH^-}(1 - \theta_1 - \theta_2) \exp[\alpha FE/RT] = k_- \theta_1 \exp[-(1 - \alpha)FE/RT] \quad (6)$$

where c_{OH^-} is the concentation of OH^- at the electrode surface, k_+ and k_- are the rate constants corresponding to the Reaction 1 or 2 in both directions, θ_1 is the degree of surface coverage by adsorbed OH and θ_2 represents any residual product on the iron surface including $Fe(OH)_2$ species. The transfer coefficient assisting the reaction in the forward direction is given by α and the rest of the symbols have the usual meaning. If one considers that hydrous $Fe(OH)_2$ is progressively blocking the electrode surface, the degree of surface coverage of the electrode (θ_T) at any instant is due to the $Fe(OH)_{ad}$ species (θ_1) and to the hydrous $Fe(OH)_2$ (θ_2) so that at $\theta_1 + \theta_2 = \theta_T$, Equation 6 can be written as

$$\theta_1 = K_1(1 - \theta_T)c_{OH^-} \exp[FE/RT] \quad (7)$$

where $K_1 = k_+/k_-$. Taking Equation 7 into account, the rate equation of Reaction 3 expressed in terms of the anodic current density (i_a) becomes

$$i_a = k'\theta_1 = k'K_1 c_{OH^-}(1 - \theta_1 - \theta_2) \exp[FE/RT] \quad (8)$$

where $k' = zFk_3$. The appearance of the current peak I during the anodic layer growth under a linear potential scan is determined by $d\theta_2/dt$. Providing that the iron electrodissolution as soluble Fe(II) is negligible as compared to the anodic layer forming process, the rate of formation of the passivating layer should be equal to the rate of the controlling step. The anodic voltammetric current density (i_a) related to the hydrous $Fe(OH)_2$ layer formation can then be expressed by the equation:

$$i_a = k'' \frac{d\theta_{Fe(OH)_2}}{dt} = k''' \frac{d\theta_{FeOH^*}}{dt} = k'\theta_1 \quad (9)$$

where k'' and k''' denote the charge densities associated with the voltammetric pseudocapacitance peaks. The kinetic relationships between both the peak height and the peak potential on v and on pH derived from equation 9 in the usual way [60–62] are

$$i_{p,I} = k'(1 - \theta_{T,p})Fv/RT \quad (10)$$

and

$$E_{p,I} = (2.303RT/F)[\log v - pH + \log k'] \quad (11)$$

Therefore the following partial derivative expressions of kinetic parameters are obtained:

$$\left(\frac{\partial \log i_{p,I}}{\partial \log v}\right)_{pH} = 1; \quad \left(\frac{\partial E_{p,I}}{\partial \log v}\right)_{pH} = 2.303RT/F$$
$$\left(\frac{\partial \log i_{p,I}}{\partial pH}\right)_{v} = 0; \quad \left(\frac{\partial E_{p,I}}{\partial pH}\right)_{v} = -2.303RT/F \quad (12)$$

The parametric relationships (12) derived from the reaction sequence (1–4) are in reasonably good agreement with those resulting from the voltammetric runs.

The complementary cathodic reaction which corresponds to the electroreduction of hydrous $Fe(OH)_2$ is associated with peak V. The latter implies a charge which is independent of v and very close to that of peak I provided that the value of $E_{s,a}$ is lower than the threshold potential of peak II. The kinetic relationships corresponding to the cathodic reaction result from the reaction sequence (1–4) in the reverse direction, namely:

$$Fe(OH)_2 + e = Fe(OH)^* + OH^- \quad (13)$$

$$Fe(OH)^* \longrightarrow Fe(OH)_{ad} \quad (14)$$

$$Fe(OH)_{ad} + e = Fe + OH^- \quad (15)$$

In this case, reactant and reaction products in the cathodic reaction are not necessarily the same proposed for the anodic process, although the reaction formalism continues to be valid. From the conventional mechanistic analysis the following relationships are obtained for the voltammetric response of the cathodic process:

$$\left(\frac{\partial \log i_{p,v}}{\partial \log v}\right)_{pH} = 1; \quad \left(\frac{\partial E_{p,v}}{\partial \log v}\right)_{pH} = -2.303RT/F$$
$$\left(\frac{\partial \log i_{p,v}}{\partial pH}\right)_{v} = 0; \quad \left(\frac{\partial E_{p,v}}{\partial pH}\right)_{v} = -2.303\ RT/F \quad (16)$$

In principle, data derived from peak V fulfil the relationships 16 (Figs 11, 12). When $E_{s,a}$ is set at a potential value where the process is influenced by that occurring at the potential of peak II (Fig. 3), the value resulting for $\partial E_{p,V}/\partial \log v$ is slightly greater than the theoretical prediction.

The interesting feature of the preceding reaction mechanism valid for the complementary reactions related to peaks I and V is that the rate determining step corresponds to a surface reaccomodation process, which should imply a weakening of the metal–metal bond and a reorientation of the surface species to facilitate the interaction of the FeOH species with the second OH^- ion required to yield $Fe(OH)_2$ through the electrochemical Reaction 4. This type of exchange place reaction has already been considered for different surface processes corresponding to the electrochemical formation of very thin layers [3, 63, 64].

4.3. *Voltammetric characteristics assigned to the growth of the passive layer*

At potentials exceeding the upper potential limit of current peak I, the anodic layer undergoes a series of complex electrochemical and chemical reactions depending on the potential scan rate and the potential limit reached in the forward sweep. These facts are clearly seen in the TMTPS results (Figs 16, 17).

The characteristics of voltammetric peak II, namely $i_{p,II}$ and $E_{p,II}$ in a range of v sufficiently low

to have the minimum overlapping with peaks I and III (Figs 1, 4) are those predicted for the electrochemical formation of an anodic layer under ohmic resistance control [50–51]. The charge related to peak II increases as $E_{s,a}$ is made more positive but, at this stage of the anodization process, ageing reactions are also involved in the overall reaction. Hence, the corresponding electroreduction profiles move in the negative potential direction when those reactions take place. The increase in thickness of the anodic layer should also imply a gradual decrease in its water content and the potential shift of the voltammogram during the backward sweep produces the shift of $E_{p,V}$. These results are related to the fact that two types of water can be distinguished in the passive film [13–15, 65] and that a small amount of boron is detected only in the outer layer formed at relative high positive potentials [17]. *In situ* studies of iron passivity using Mössbauer and EXAFS spectroscopy show significant changes in the direction of crystallization upon removal from solution and subsequent long term drying of the iron sample [66].

Voltammetric peaks III and IV change only slightly during the potential cycling. Consequently, no accumulation of charge is detected as was the case in strongly alkaline solution [40]. The two-layer structure model developed by Cohen [1–6] and Sato [11–19] for the passive layer on iron in aqueous solutions, based on an inner and an outer layer where the former approaches the structure of Fe_3O_4 at high positive potentials, was taken into account. The conclusion from the results shown in Figs 4 and 5 is that the outer structure, which is responsible for the accumulation of charge in strong alkaline solutions, exhibits a rate of growth which gradually decreases as the solution pH decreases. The duplex structure of the passive film on iron was also recently deduced from *in situ* photoacoustic spectroscopy [69].

The reactions related to peaks III and IV apparently take place at the outer porous hydrous iron oxy-hydroxide layer. The structure of this layer at a constant pH is also influenced by the composition of the electrolyte solution. This is apparently confirmed by voltammetric runs under potential perturbation conditions such that only the outer hydrous iron oxy-hydroxide layer is involved in the electrochemical reaction (Fe(II)/Fe(III) redox system). In this case the voltammogram resembles that obtained with an electrode formed with hydrous iron hydroxide precipitated on an electrochemically inert conducting substrate [67, 68].

Acknowledgements

INIFTA is a research institute jointly established by the Universidad Nacional de La Plata, the Consejo Nacional de Investigaciones Científicas y Técnicas and the Comisión de Investigaciones Científicas de la Provincia de Buenos Aires. Part of the equipment used in the present work was provided through the Cooperation Agreement between the University of Mainz (Germany) and the University of La Plata (Argentina).

References

[1] M. Nagayama and M. Cohen, *J. Electrochem. Soc.* **109** (1962) 781.
[2] *Idem, ibid,* **110** (1963) 670.
[3] N. Sato and M. Cohen, *ibid.* **111** (1964) 512, 519, 624.
[4] V. Markovac and M. Cohen, *ibid.* **114** (1967) 674.
[5] M. Cohen and K. Hashimoto, *ibid.* **121** (1974) 42.
[6] M. Cohen, D. Mitchell and K. Hashimoto, *ibid.* **126** (1979) 442.
[7] J. Kruger and J. P. Calvert, *ibid.* **114** (1967) 43
[8] C. L. Foley, J. Kruger and C. J. Bechtoldt, *ibid.* **114** (1967) 994.
[9] R. V. Moshtev, *Ber. Bunsenges. Phys. Chem.* **71** (1967) 1079.
[10] *Idem, ibid.* **72** (1968) 452
[11] N. Sato and T. Notoya, *Denki-Kagaku* **35** (1967) 100.
[12] N. Sato and K. Kudo, *Electrochim. Acta* **16** (1971) 447.
[13] N. Sato, K. Kudo and T. Noda, *Electrochim. Acta* **16** (1971) 1909.
[14] *Idem, Z. Phys. Chem. N.F.* **98** (1975) 271.
[15] *Idem, J. Jpn. Inst. Met.* **37** (1973) 951.

[16] N. Sato, K. Kudo and R. Nishimura, *J. Electrochem. Soc.* **123** (1976) 1419.
[17] M. Seo, N. Sato, J. B. Lumsden and R. W. Staehle, *Corros. Sci.* **17** (1977) 209.
[18] T. Ohtsuka, K. Azumi and N. Sato, 'Passivity of Metals and Semiconductors' (edited by M. Froment), Elsevier, Amsterdam (1983) pp. 199–203.
[19] R. Nishimura and N. Sato, 'Proc. 9th Int. Congr. Met. Corrosion, Toronto', Vol. 1, National Research Council of Canada, Ottawa (1984) pp. 96–101.
[20] J. L. Ord, *J. Electrochem. Soc.* **113** (1966) 213.
[21] *Idem,* 'Passivity of Metals' (edited by R. P. Frankenthal and J. Kruger), The Electrochemical Society, Princeton, (1978) pp. 273–284.
[22] *Idem,* 'Passivity of Metals and Semiconductors' (edited by M. Froment), Elsevier, Amsterdam (1983) pp. 95–100.
[23] J. L. Ord and D. J. DeSmet, *J. Electrochem. Soc.* **113** (1966) 1253.
[24] *Idem, ibid.* **118** (1971) 206.
[25] *Idem, ibid.* **123** (1976) 1876.
[26] F. C. Ho and J. L. Ord, *ibid.* **119** (1972) 139.
[27] J. O'M. Bockris, M. A. Genshaw and V. Brusic, *Symp. Faraday Soc.* **4** (1970) 177.
[28] J. O'M. Bockris, M. A. Genshaw, V. Brusic and H. Wroblowa, *Electrochim. Acta* **16** (1971) 1859.
[29] R. W. Revie, B. G. Baker and J. O'M. Bockris, *J. Electrochem. Soc.* **122** (1975) 1460.
[30] J. O'M. Bockris, O. J. Murphy and D. L. Cocke, *ibid.* **129** (1982) 1276.
[31] O. J. Murphy, J. O'M. Bockris, T. E. Pou, D. L. Cocke and G. Sparrow, *ibid.* **129** (1982) 2149.
[32] O. J. Murphy, T. E. Pou, J. O'M. Bockris and L. L. Tongsen, *ibid.* **131** (1984) 2785.
[33] G. T. Burstein and G. W. Ashley, *Corrosion* **39** (1983) 241.
[34] G. T. Burstein and D. H. Davies, *Corros. Sci.* **20** (1980) 1143.
[35] *Idem, J. Electrochem. Soc.* **128** (1981) 33.
[36] R. S. Schrebler Guzman, J. R. Vilche and A. J. Arvia, *J. Appl. Electrochem.* **11** (1981) 551.
[37] *Idem, Anal. Asoc. Quim. Arg.* **70** (1982) 999.
[38] J. O. Zerbino, J. R. Vilche and A. J. Arvia, *J. Appl. Electrochem.* **11** (1981) 703.
[39] D. M. Drazic and C. S. Hao, *Glasnik Hem. društva Beograd* **47** (1982) 649.
[40] R. S. Schrebler Guzman, J. R. Vilche and A. J. Arvia, *Electrochim. Acta* **24** (1979) 395.
[41] J. R. Vilche and A. J. Arvia, *Acta Cientif. Venez.* **31** (1980) 408.
[42] M. E. Vela, J. R. Vilche and A. J. Arvia, 'Passivity of Metals and Semiconductors' (edited by M. Froment), Elsevier, Amsterdam (1983) pp. 59–65.
[43] D. D. Macdonald and D. Owen, *J. Electrochem. Soc.* **120** (1976) 1691.
[44] L. Ojefors, *ibid.* **123** (1976) 1691.
[45] T. R. Jayarman, V. K. Vendatesan and H. V. K. Udupa, *Electrochim. Acta* **20** (1975) 209.
[46] H. Gomez Meier, J. R. Vilche and A. J. Arvia, *J. Electroanal. Chem.* **138** (1982) 367.
[47] D. M. Drazic and C. S. Hao, *Electrochim. Acta* **27** (1982) 1409.
[48] H. Schweickert, W. J. Lorenz and H. Friedberg, *J. Electrochem. Soc.* **127** (1980) 1693.
[49] M. Keddam, O. R. Mattos and H. Takenouti, *ibid.* **128** (1981) 257, 266.
[50] A. J. Calandra, N. R. de Tacconi, R. Pereiro and A. J. Arvia, *Electrochim. Acta* **19** (1974) 901.
[51] D. D. Macdonald, 'Transient Techniques in Electrochemistry', Plenum Press, New York (1977).
[52] J. R. Vilche and A. J. Arvia, *Anal. Acad. Cs, Ex. Fis. Nat. Buenos Aires* **33** (1981) 33.
[53] A. J. Arvia, 'Proc. 8th Inter. Congr. Met. Corros.' Mainz, Vol. 3, DECHEMA, Frankfurt (1981) pp. 2065–2080.
[54] M. Froelicher, A. Hugot-Le Goff and V. Javanicevic, 'Passivity of Metals and Semiconductors' (edited by M. Froment), Elsevier, Amsterdam (1983) pp. 85–88; 491–495.
[55] Z. Szklarska-Smialowska and W. Kozlowski, *J. Electrochem. Soc.* **131** (1984) 234, 499.
[56] B. Agius and J. Siejka, *ibid.* **120** (1973) 1019.
[57] A. B. Anderson and N. K. Ray, *J. Phys. Chem.* **86** (1982) 488.
[58] M. Pourbaix, 'Atlas of Electrochemical Equilibria in Aqueous Solutions', Pergamon-CEBELCOR, Brussels (1966).
[59] R. P. Frankenthal, *Electrochim. Acta* **16** (1971) 1845.
[60] S. Srinivasan and E. Gileadi, *ibid.* **11** (1966) 321.
[61] H. Angerstein-Kozlowska, J. Klinger and B. E. Conway, *J. Electroanal. Chem.* **75** (1977) 45, 61.
[62] R. S. Schrebler Guzman, J. R. Vilche and A. J. Arvia, *Corros. Sci.* **18** (1978) 765.
[63] A. M. Lanyon and B. M. W. Trapnell, *Proc. Royal Soc.* **A227** (1955) 387.
[64] V. Brusic, 'Oxides and Oxide Films', Vol. 1 (edited by J. W. Diggle), Marcel Dekker, New York (1972) pp. 1–89.
[65] M. C. Bloom and L. Goldenberg, *Corros. Sci.* **5** (1965) 623.
[66] R. W. Hoffman, 'Passivity of Metals and Semiconductors (edited by M. Froment), Elsevier, Amsterdam (1983) pp. 147–162.
[67] V. A. Macagno, J. R. Vilche and A. J. Arvia, *J. Appl. Electrochem.* **11** (1981) 417.
[68] M. E. Vela, J. R. Vilche and A. J. Arvia, *Electrochim. Acta,* submitted.
[69] K. Ogura, A. Fujishima and K. Houda, *J. Electrochem. Soc.* **131** (1984) 344.